Dual-Band Wide-Angle Circularly-Polarized Microstrip Antenna by Ferrite Ring Inserted in Its Cavity Domain

Fazel Rangriz Rostami [1], Gholamreza Moradi [1,2], and Reza Sarraf Shirazi [1]

[1,2,3] Department of Electrical Engineering
Amirkabir University of Technology, Tehran, Iran
fazel.rangriz@aut.ac.ir, ghmoradi@aut.ac.ir, sarraf@aut.ac.ir

[2] Department of Mechanical Engineering
University of Alberta, Alberta, Canada

Abstract ─ In this paper coaxially-fed circular microstrip patch antenna with ferrite ring in its cavity domain is presented in order to obtain dual-band circularly-polarized antenna in X-band having wide angle axial ratio in both bands. A mode matching approach is used to see the effects of each mode on input impedance of the antenna and is validated numerically by finite element method. The theoretical calculations for input impedance are in good agreement with full-wave simulation. The scattering and radiation parameters of the antenna are investigated. The antenna patch radius and height are 8 and 1 mm, respectively. The ferrite ring was made of yttrium iron garnet (YIG) and the substrate of antenna is Rogers RT5880. In the first band the antenna has 7 dB gain and the ratio of Copol/Xpol is about 24 dB and in the second band has 5 dB gain and the XPD, i.e., the ratio of Copol to Xpol is about 20 dB.

Index Terms ─ Dual-band circularly-polarized antenna, microstrip antennas, mode-matching, wide-angle antenna.

I. INTRODUCTION

Circular polarization (CP) is extensively used in wireless and satellite communications. In many papers, ferrite substrate was used to generate CP [1]-[2]. In [3], circularly polarized microstrip antenna based on the unidirectional resonant modes of a ferrite disk has been introduced which produce wide angle circular polarization for GPS application. In [4], circularly polarized microstrip antenna has been obtained by small ferrite disks inserted in its cavity domain. In order to have single-feed dual-band CP antenna various configurations have been investigated for GPS application [5]-[6]. A compact CP dual-band antenna was successfully designed for Meteosat satellite in L and X communication bands [7]. In [8], a compact dual-band CP multilayer microstrip antenna using LTCC technology has been proposed and implemented, due to the stacked-patch structure and inserted slits, the designed antenna has a small volume compared to the conventional dual-band CP antennas. A crossed asymmetric dipole antenna over a dual-band AMC surface has been introduced in [9] in which, the proposed antenna yields a low profile, good impedance matching, good CP radiation, and an improved 3-dB AR bandwidth at both operating bands. Sun *et al.* have introduced a dual-feed stacked annular-ring patch antenna which is dual-band, dual-layer; and is excited by two orthogonal H-shaped slots, fed by a 3-dB hybrid [10]. In [4], it is shown that dual-band CP antennas can be obtained by insertion of two or more ferrite disks in the cavity region of the antenna along with appropriate optimization of the bias magnetic field.

In this letter, a new configuration to achieve single-feed dual-band CP microstrip antenna is presented. Antenna has been excited via coaxial port; in addition, a ferrite ring is inserted in antenna cavity domain in order to produce circular polarization.

This paper is organized as follows. Section II introduces the structure of complete antenna. The theoretical analysis of input impedance of antenna is described in Section III and the results are validated by full-wave simulations and discussed. In Section IV radiation characteristics of antenna are simulated with CST Studio and discussed.

II. ANTENNA STRUCTURE

Figure 1 (a) shows the proposed antenna, which consists of a ferrite ring inserted in the cavity domain of the substrate. The ferrite disk is magnetized normal to the ground plane by a dc bias magnetic field H_0, which can be provided by a permanent magnet placed underneath the ground plane. The substrate of antenna is made of RT5880, permeability (μ) of the substrate is equal to that of the air, i.e., $\mu = \mu_0$, and has relative permittivity 2.2 and its loss tangent $\tan(\delta)$ is about 0.0009. The cavity domain of antenna has four regions as it can be seen from Fig. 1 (b). Region I is defined by

Submitted On: July 14, 2016
Accepted On: November 19, 2016

$0 < r < a$, which is from the center of the patch to the current probe that is fed at $r = a$. Region II is defined by $a < r < b$. This region is between feed probe and ferrite ring. Region III is defined by $b < r < c$, which contains ferrite ring, and finally, region IV is defined by $c < r < d$, which is between ferrite ring and edge of the patch. The ferrite ring with thickness 1 mm and height 1 mm is inserted in the cavity domain of patch antenna with radius 8 mm, and its substrate height is 1 mm.

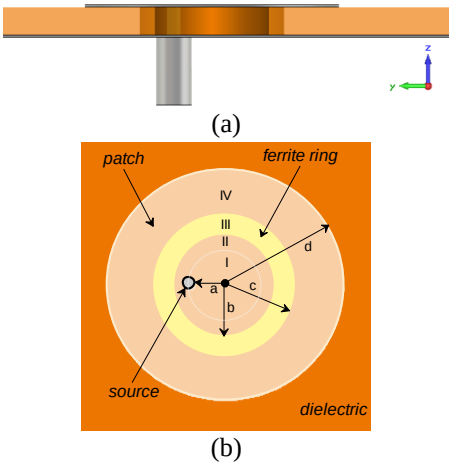

Fig. 1. (a) Side view of the antenna, and (b) top view of the antenna.

Permeability of the ferrite ring is defined as the following:

$$\mu = 1 + \frac{(\omega_H + j\,\omega\alpha)\omega_M}{\left(\omega_H + j\,\omega\alpha\right)^2 - \omega^2}, \tag{1}$$

$$\mu_a = \frac{\omega_M\,\omega}{\left(\omega_H + j\,\omega\alpha\right)^2 - \omega^2}, \tag{2}$$

$$\mu_\perp = \mu - \frac{\mu_\alpha^2}{\mu}, \tag{3}$$

in which μ and μ_α are the diagonals and off-diagonal elements of the permeability tensor of the ferrite, respectively, where $\omega_H = \gamma H_0$ and $\omega_M = \gamma M_s$, with M_s the saturation magnetization of the ferrite, and γ the gyromagnetic ratio, and also α is the Gilbert damping constant, and $\left(\Delta H = 2\alpha\omega/\gamma\right)$ is magnetic line width of the ferrite material, and also $\mu_\perp$ is effective permeability of ferrite material. The material properties of the ferrite ring are according to the Table 1.

Table 1: Ferrite material properties

H_0	ΔH	$4\pi M_s$	ε_{fer}
600 (Oe	20 (Oe)	1780 (Gauss)	15

Real and imaginary parts of ferrite permeability in desired frequency range are plotted in Fig. 2.

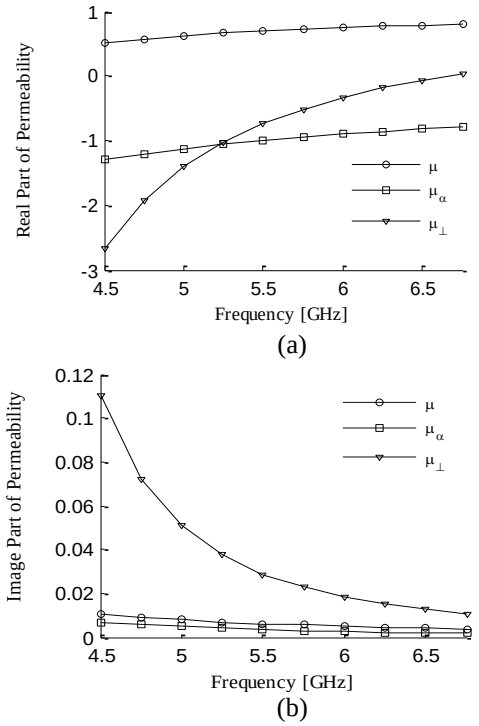

Fig. 2. Permeability of ferrite: (a) real part, and (b) imaginary part. Ferrite parameters are the same as Table 1.

III. INPUT IMPEDANCE

To determine the input impedance of the antenna, it is necessary to find the field solution beneath the circular patch. In general, these solutions take the form of a cylindrical mode expansion, with each mode being determined by arbitrary constants. To find all of these constants, additional boundary conditions are required, which are obtained by considering the wall admittances. The electric and magnetic field solution in each region can be written as following, in which for simplification purposes, the variations of the fields in z direction are ignored:

$$E_z^I(r,\phi) = \sum_n -j\omega A_n e^{jn\phi} J_n(kr), \tag{4}$$

$$H_\phi^I(r,\phi) = \sum_n -A_n \frac{1}{\mu_0} e^{jn\phi} \frac{\partial}{\partial r} J_n(kr), \tag{5}$$

$$E_z^{II}(r,\phi) = \sum_n -j\omega e^{jn\phi} \left(B_n J_n(kr) + C_n Y_n(kr)\right), \tag{6}$$

$$H_\phi^{II}(r,\phi) = \sum_n -\frac{1}{\mu_0} e^{jn\phi} \left(B_n \frac{\partial}{\partial r} J_n(kr) + C_n \frac{\partial}{\partial r} Y_n(kr)\right), \tag{7}$$

where J_n and Y_n are Bessel function of the first kind and second kind, respectively. In region I, II and IV, we have ordinary substrate and $k = k_0\sqrt{\varepsilon_r}$ in which, k_0 is

the free space wave number. In region III, due to the presence of the ferrite material electric and magnetic fields are written as following:

$$E_z^{III}(r,\phi)=\sum_n -j\omega e^{jn\phi}\left(D_n J_n(k_\perp r)+E_n Y_n(k_\perp r)\right), \quad (8)$$

$$H_\phi^{III}(r,\phi)=\sum_n -\frac{j}{\mu_0}e^{jn\phi}\left(\frac{\mu r\frac{\partial}{\partial r}E_z^{III}(r,\phi)+n\mu_\alpha E_z^{III}(r,\phi)}{\omega r\mu_\perp}\right), \quad (9)$$

in which $k_\perp = k_0\sqrt{\varepsilon_{fer}\mu_\perp}$. In region IV, we have the next ordinary substrate, will then result to:

$$E_z^{IV}(r,\phi)=\sum_n -j\omega e^{jn\phi}\left(F_n J_n(kr)+G_n Y_n(kr)\right), \quad (10)$$

$$H_\phi^{IV}(r,\phi)=\sum_n -\frac{1}{\mu_0}e^{jn\phi}\left(F_n\frac{\partial}{\partial r}J_n(kr)+G_n\frac{\partial}{\partial r}Y_n(kr)\right). \quad (11)$$

In order to take the feed probe into account, neglecting the variation of the probe current in the $z-$ direction, an infinitely thin electric current line source carrying a constant current I_0 is assumed. The current density of the line source is:

$$\boldsymbol{J}=\hat{z}\,J_z=\hat{z}\frac{I_0}{r_0}\delta(r-a)\delta(\phi).$$

Boundary conditions on the tangential components of the electric and magnetic fields are applied as following:

$$E_z^I(a,\phi)=E_z^{II}(a,\phi), \quad (12)$$

$$H_\phi^{II}(a,\phi)-H_\phi^I(a,\phi)=J_z, \quad (13)$$

$$E_z^{II}(b,\phi)=E_z^{III}(b,\phi), \quad (14)$$

$$H_\phi^{II}(b,\phi)=H_\phi^{III}(b,\phi), \quad (15)$$

$$E_z^{III}(c,\phi)=E_z^{IV}(c,\phi), \quad (16)$$

$$H_\phi^{III}(c,\phi)=H_\phi^{IV}(c,\phi). \quad (17)$$

By considering wall admittance on the side wall of the microstrip antenna, the next boundary condition can be written as following:

$$H_\phi^{IV}(d,\phi)=-y_n E_z^{IV}(d,\phi). \quad (18)$$

By using Equations (11) through (17), the constants A_n, B_n, C_n, D_n, E_n, F_n, and G_n will be evaluated. The input impedance can be written as following:

$$Z_{in}=-\frac{1}{I_0}\int_0^h E_z^I(r=a,\phi=0)dz. \quad (19)$$

In this paper the wall admittance, described in [11] is used, this wall admittance y_n fix the ratio between the $z-$directed electric field and the $\phi-$directed magnetic field for each mode. The antenna parameters are considered as Table 2.

Table 2: Antenna parameters

a	*b*	*c*	*d*
2.5 mm	4 mm	5 mm	8 mm

In the absence of ferrite ring, the superposition of two azimuthally travelling waves in opposite direction, have the same amplitude and resonance frequency, results in a standing wave behavior of the electric field. In order to show the effect of ferrite ring on the separation of resonance frequency of the right-handed and left-handed azimuthal modes, input impedance of each mode is individually plotted in Fig. 3. As it can be seen, modes of $n=\pm1$ do not have the same resonance frequency. These two modes have the most influence on the input impedance, and the other modes have a negligible effect on the real part of input impedance but increase the imaginary part of the input impedance.

Figures 4 and 5 show the comparison between our theoretical results for the input impedance and return loss, and those obtained by CST studio full wave simulator. For each calculation, we have considered 5 modes, the modes having order of greater than 5 were found to have insignificant effect on the calculated input impedance. It is seen that the mode matching results are close to that obtained by the CST studio simulation. The antenna has impedance bandwidth between (5.26 GHz-5.34 GHz) or 1.5% and (6 GHz-6.2 GHz) or 1.7% in first and second band, respectively.

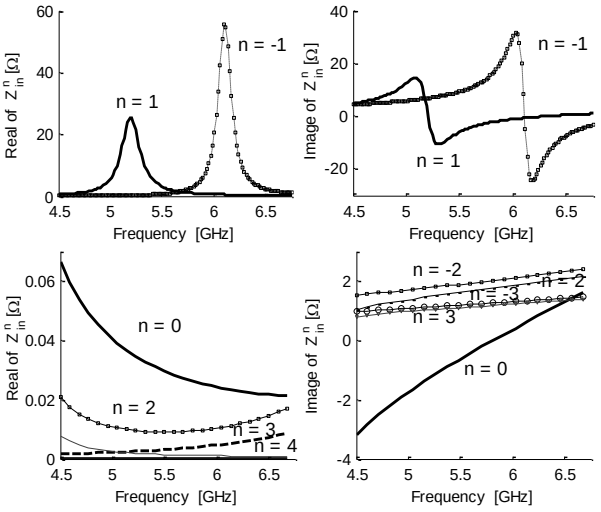

Fig. 3. Input impedance of each mode.

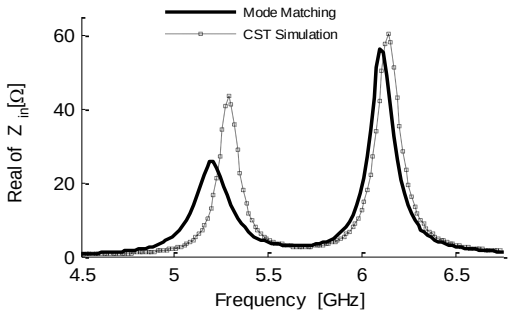

(a)

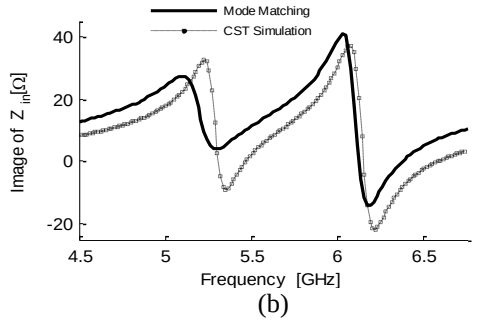

(b)

Fig. 4. Comparison between mode matching method and CST studio results: (a) real part and (b) imaginary part.

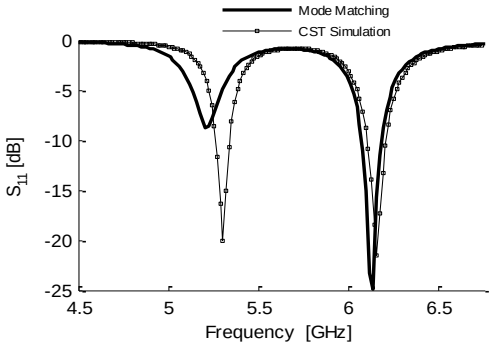

Fig. 5. Comparison of return loss between mode matching method and CST studio results.

The proposed dual-band CP antenna can be designed by adjusting the thickness of ferrite ring and by varying the dc bias field H_0 of ferrite.

Figure 6 shows the effect of ring thickness on the first and second band resonance frequency. By increasing the ring thickness, both resonance frequencies decrease which is due to the increasing of the effective permittivity and permeability of the substrate. Also, the separation between two resonance frequencies increases because the ferrite region which has anisotropic behavior is increased.

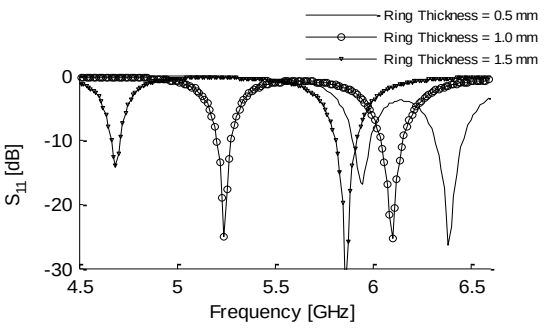

Fig. 6. Full-wave simulation result of the return loss against the ring thickness. The other design parameters are the same as in Fig. 4.

Figure 7 shows the effect of dc bias field H_0 on the resonance frequency. As it can be seen, by increasing the bias field, the resonance frequencies, and especially the second can be controlled.

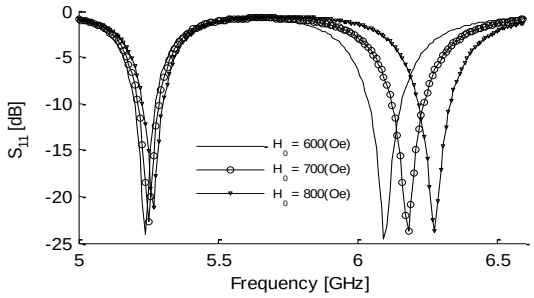

Fig. 7. Full-wave simulation result of the return loss against the magnetic bias field. The other design parameters are the same as in Fig. 4.

IV. RADIATION PROPERTIES

In order to examine radiation properties of the antenna, we consider a structure whose patch and ground plane are made of copper and having thickness of 50 microns. The ground dimensions in full wave simulation are considered $60\times60\ mm^2$.

Figure 8 shows the simulation results of axial ratio of the antenna on broadside direction versus frequency. As it can be seen, 3 dB axial ratio at first and second band is between (5.06 GHz-5.42 GHz) or 6.87% and (6.04 GHz-6.27 GHz) or 3.74%, respectively. The axial ratio bandwidth is wider than the impedance bandwidth which is given in Fig. 5. In Fig. 9, simulated axial ratio of the proposed antenna versus θ, at the first and second resonance frequencies are shown, the wide angle behavior of the antenna can be seen in this figure.

In Fig. 10, the gain of the antenna as a function of frequency is shown, the antenna has 7 dB gain in first band and 5 dB gain in second band.

In Fig. 11, simulated radiation patterns for RHCP and LHCP at first and second resonance frequency in the XOZ plane ($\phi=0$) and YOZ ($\phi=90$) plane are shown.

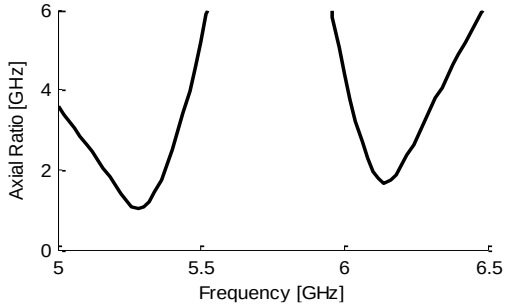

Fig. 8. The simulated broadside axial ratio versus frequency.

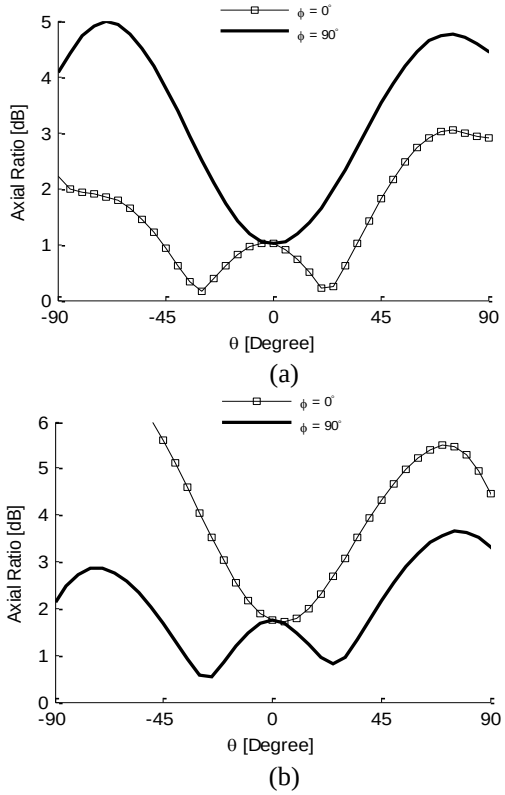

Fig. 9. Simulated axial ratio of the proposed antenna versus θ: (a) 5.3 GHz and (b) 6.16 GHz.

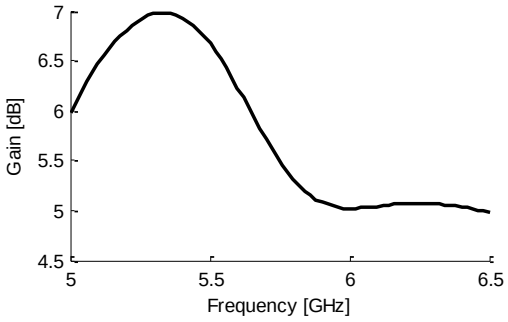

Fig. 10. The simulated broadside gain versus frequency.

It can be observed that the antenna has LHCP polarization in the first band and RHCP polarization in the second band. The Co-pol/Xpol is about 24 dB and 20 dB in the first and second bands, respectively. It is noticeable that the state of polarization can be switched by reversing the direction of the DC magnetic bias field. The efficiency of the antenna in first and second bands are 90% and 60%, respectively. The decrease in efficiency of the second band is due to the increase in ferrite loss. In Fig. 12, the loss of each part the antenna is plotted as a function of frequency. Here, the total input power in full-wave simulation is 500 mW. As it can be seen, the loss of ferrite ring is more than other losses and it plays the major role in antenna efficiency.

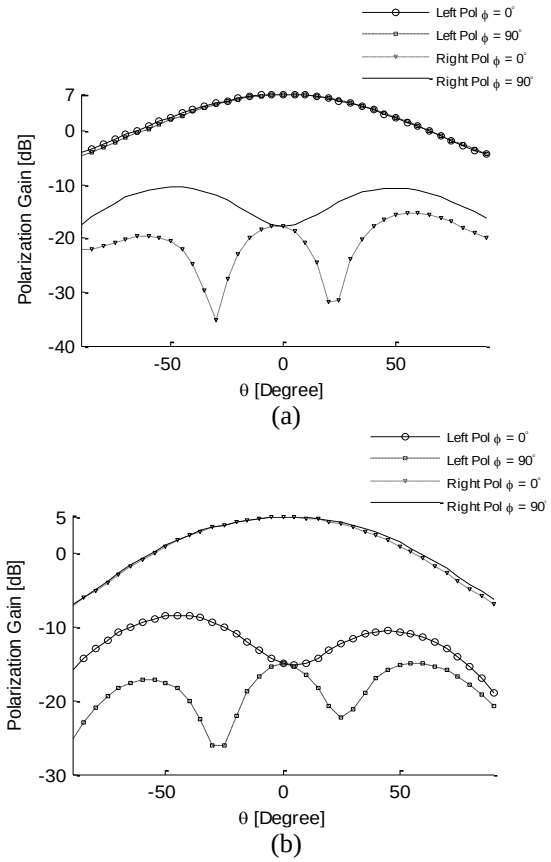

Fig. 11. Simulated radiation patterns for RHCP and LHCP at 5.3 GHz and 6.16 GHz in the XOZ plane ($\phi = 0$) and YOZ ($\phi = 90$) plane: (a) 5.3 GHz and (b) 6.16 GHz.

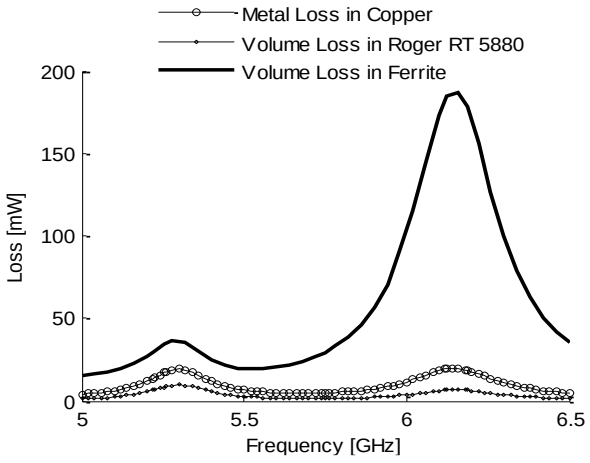

Fig. 12. Loss in each part of the antenna (total input power is 500 [mW])

V. CONCLUSION

A new single-layer single-feed dual-band CP antenna with wide-angle axial ratio in both frequency bands by inserting a ferrite ring in cavity domain has been proposed. This antenna has 6.87% axial ratio bandwidth, and 1.5% impedance bandwidth in the first band. It also has 3.74% axial ratio bandwidth and 1.7% impedance bandwidth in the second band and can be used as a frequency tunable antenna. Proposed structure is compact, easy to design and fabricate, and does not require a complicated feeding network. Therefore, it could be a good candidate for realizing wide-angle dual-band CP antennas.

REFERENCES

[1] D. M. Pozar, "Radiation and scattering characteristics of microstrip antennas on normally biased ferrite substrates," in *IEEE Transactions on Antennas and Propagation*, vol. 40, no. 9, pp. 1084-1092, Sep. 1992.

[2] A. D. Brown, J. L. Volakis, L. C. Kempel, and Y. Botros, "Patch antennas on ferromagnetic subtrates," in *IEEE Transactions on Antennas and Propagation*, vol. 47, no. 1, pp. 26-32, Jan. 1999.

[3] J. Ghalibafan, B. Rejaei, and N. Komjani, "A circlarly polarized antenna based on the unidirectional resonant modes of a Ferrite disk," in *IEEE Transactions on Magnetics*, vol. 50, no. 3, pp. 88-95, Mar. 2014.

[4] M. Sigalov, R. Shavit, R. Joffe and E. O. Kamenetskii, "Manipulation of the radiation characteristics of a patch antenna by small Ferrite disks inserted in its cavity domain," in *IEEE Transactions on Antennas and Propagation*, vol. 61, no. 5, pp. 2371-2379, May 2013.

[5] W. T. Hsieh, T. H. Chang, and J. F. Kiang, "Dual-band circularly polarized cavity-backed annular slot antenna for GPS receiver," in *IEEE Transactions on Antennas and Propagation*, vol. 60, no. 4, pp. 2076-2080, Apr. 2012.

[6] M. Maqsood, et al., "Low-cost dual-band circularly polarized switched-beam array for global navigation satellite system," in *IEEE Transactions on Antennas and Propagation*, vol. 62, no. 4, pp. 1975-1982, Apr. 2014.

[7] F. Ferrero, C. Luxey, G. Jacquemod, and R. Staraj, "Dual-band circularly polarized microstrip antenna for satellite applications," in *IEEE Antennas and Wireless Propagation Letters*, vol. 4, no. , pp. 13-15, 2005.

[8] K. Qian and X. Tang, "Compact LTCC dual-band circularly polarized perturbed hexagonal microstrip antenna," in *IEEE Antennas and Wireless Propagation Letters*, vol. 10, pp. 1212-1215, 2011.

[9] S. X. Ta and I. Park, "Dual-band low-profile crossed asymmetric dipole antenna on dual-band AMC surface," in *IEEE Antennas and Wireless Propagation Letters*, vol. 13, pp. 587-590, 2014.

[10] X. Sun, Z. Zhang, and Z. Feng, "Dual-band circularly polarized stacked annular-ring patch antenna for GPS application," in *IEEE Antennas and Wireless Propagation Letters*, vol. 10, pp. 49-52, 2011.

[11] F. R. Rostami, G. Moradi, and R. S. Shirazi, "Mode matching in microstrip antenna with both electric and magnetic surface current on sidewall in cavity model," *Applied Computational Electromagnetics Society Journal*, vol. 31, no. 7, 2016.